Longitudinal development of hippocampal subregions from childhood to adulthood

Running head: Development of hippocampal subregions

Christian K. Tamnes[1], Marieke G. N. Bos[2,3], Ferdi C. van de Kamp[2], Sabine Peters[2,3], and Eveline A. Crone[2,3]

[1] Department of Psychology, University of Oslo, Oslo, Norway

[2] Institute of Psychology, Leiden University, Leiden, The Netherlands

[3] Leiden Institute for Brain and Cognition, Leiden, The Netherlands

Corresponding author: Christian K. Tamnes, Department of Psychology, University of Oslo, PO Box 1094 Blindern, 0317 Oslo, Norway; Email: c.k.tamnes@psykologi.uio.no

Conflict of Interest: The authors declare no competing financial interests.

Acknowledgements: This study was supported by the Research Council of Norway and the University of Oslo (FRIMEDBIO 230345 to CKT), and the European Research Council Starting Grant scheme (ERC-2010-StG_263234 to EAC).

Highlights

- Hippocampal subregions develop in differential ways from childhood to adulthood
- Subiculum, CA1, ML and fimbria showed nonlinear trajectories with initial increases
- Parasubiculum, presubiculum, CA2/3, CA4 and GC-DG showed linear volume decreases
- There were no sex differences in hippocampal subregion development
- General cognitive ability associated with CA2/3 and CA4 volumes and ML development

Abstract

Detailed descriptions of the development of the hippocampus promise to shed light on the neural foundation of development of memory and other cognitive functions, as well as the emergence of major mental disorders. Hippocampus is a heterogeneous structure with a well characterized internal complexity, but development of its distinct subregions in humans has remained poorly described. We analyzed magnetic resonance imaging (MRI) data from a large longitudinal sample (270 participants, 678 scans) using an automated segmentation tool and mixed models to delineate the development of hippocampal subregion volumes from childhood to adulthood. We also investigated whether subregion volumes and development were sexually dimorphic and related to general cognitive ability. Nonlinear developmental trajectories with early volume increases were observed for subiculum, cornu ammonis (CA) 1, molecular layer (ML) and fimbria. In contrast, parasubiculum, presubiculum, CA2/3, CA4 and the granule cell layer of the dentate gyrus (GC-DG) showed linear volume decreases. No sex differences were found in hippocampal subregion development. Finally, general cognitive ability was positively associated with CA2/3 and CA4 volumes, as well as with ML development. In conclusion, hippocampal subregions appear to develop in diversified ways across adolescence, and specific subregions link to general cognitive level.

Keywords: adolescence; brain development; general cognitive ability; hippocampus; MRI; subfields

Introduction

Knowledge of the development of the hippocampus from childhood to adulthood is important for understanding the neural foundation of development of cognitive functions, including episodic memory (Ghetti & Bunge, 2012; Østby, Tamnes, Fjell, & Walhovd, 2012). Moreover, it may offer insight into the origin and ontogeny of major mental disorders including schizophrenia and depression, which frequently emerge in adolescence (Lee, Heimer, et al., 2014; Whiteford et al., 2013), and for which the hippocampus appears to be a key node in the underlying distributed brain networks (Schmaal et al., 2016; van Erp et al., 2016). Magnetic resonance imaging (MRI) studies have investigated cross-sectional age-related differences or longitudinal changes in hippocampal volume in children and adolescents. The hippocampus is however not a uniform structure, but contains anatomically and functionally distinct regions (Amaral & Lavenex, 2007). It is thus possible that different subregions develop differently.

Hippocampal volume increases during childhood (Brown et al., 2012; Gilmore et al., 2012; Hu, Pruessner, Coupe, & Collins, 2013; Swagerman, Brouwer, de Geus, Hulshoff Pol, & Boomsma, 2014; Uematsu et al., 2012), but results for the adolescent period have been more variable. Several cross-sectional studies (Koolschijn & Crone, 2013; Muftuler et al., 2011; Yurgelun-Todd, Killgore, & Cintron, 2003; Østby et al., 2009) and some longitudinal studies (Mattai et al., 2011; Sullivan et al., 2011) found no significant age effects. More recent longitudinal studies have found volume increase (Dennison et al., 2013), decrease (Tamnes et al., 2013), or a quadratic inverted U-shaped trajectory (Narvacan, Treit, Camicioli, Martin, & Beaulieu, 2017; Wierenga et al., 2014). The latter finding is supported by a recent multisite longitudinal developmental study (Herting et al., in press) and a large cross-sectional lifespan study (Coupe, Catheline, Lanuza, Manjon, & Alzheimer's Disease Neuroimaging Initiative, 2017).

Estimating whole hippocampal volume may however mask regional developmental differences. Anatomically, the hippocampus is a unique structure consisting of cytoarchitectonically distinct subregions, including the cornu ammonis (CA) subfields, the dentate gyrus (DG) and the subicular complex (Insausti & Amaral, 2012). The hippocampal formation also has a unique set of largely unidirectional, excitatory pathways along the transverse plane (Amaral & Lavenex, 2007). Despite this well characterized internal complexity, researchers studying the human hippocampus *in vivo* have traditionally modelled and measured it as a whole (but see (Insausti, Cebada-Sanchez, & Marcos, 2010)). Novel protocols to segment the hippocampal subregions in MRI images have

however been developed. Analysis of subregion within the hippocampus may unravel heterogeneous developmental patterns with differential functional relevance.

A pioneer study indicated different developmental changes in subareas of the hippocampus, mainly with increases over time in posterior areas and decreases in anterior areas (Gogtay et al., 2006). This was partly supported by a study investigating age-related differences in the head, body and tail of the hippocampus, finding an increase in the volume of the body, in contrast to decreases in the right head and tail (DeMaster, Pathman, Lee, & Ghetti, 2014). Other studies have investigating the development of more clearly defined hippocampal subregions, including its subfields. In a large cross-sectional study, Krogsrud et al. (2014) found that most subregions showed age-related volume increases from early childhood until approximately 13-15 years, followed by little differences. For a subsample of the older participants from this study, Tamnes et al. (2014) performed a longitudinal follow-up and found that change rates were different across subregions, but that nearly all showed small volume decreases in the teenage years. Combined, these results fit with the observed inverted U-shaped trajectory for whole hippocampal volume. Based on manual segmentation of subfields in the hippocampus body, Lee et al. (2014) found age-related increases in the right CA1 and CA3/DG volumes into early adolescence. Finally, in a lifespan sample, Daugherty et al. (2016) performed manual tracing on slices in the anterior hippocampus body and found negative relationships with age during development for CA1/2 and CA3/DG volumes.

Together, these results suggest that hippocampal subregions may continue to change in subtle and diverse ways through both childhood and adolescence, but the available studies have major limitations. First, the samples sizes were mostly small (only (Krogsrud et al., 2014) included >100 children and adolescents). Second, only two of the previous studies had longitudinal data (Gogtay et al., 2006; Tamnes et al., 2014) and could investigate growth trajectories. Third, two of the previous studies (Krogsrud et al., 2014; Tamnes et al., 2014) used an automated segmentation procedure (Van Leemput et al., 2009) for which the reliability and validity has later been challenged (de Flores et al., 2015; Wisse, Biessels, & Geerlings, 2014), and these results have to be interpreted with caution. The other two studies of specific subregions (Daugherty et al., 2016; Lee, Ekstrom, et al., 2014) used manual tracing protocols (Ekstrom et al., 2009; Mueller et al., 2007) which yield estimates of a smaller number regions measured only in the hippocampal body. Moreover, although manual segmentation certainly has its advantages, it is laborious and can be infeasible for large longitudinal studies, and also requires some subjectivity and is thus vulnerable to bias (Schlichting, Mack, Guarine, & Preston, 2017). The manual methods are thus not optimal in the context of the

increasing focus on larger samples to obtain adequate statistical power (Button et al., 2013; Nord, Valton, Wood, & Roiser, 2017) and replication (Open Science Collaboration, 2015).

We aimed to address these shortcomings by analyzing data from a large new longitudinal sample of 270 participants with 678 MRI scans in the age-range 8-28 years using a novel automated segmentation tool. Specifically, we aimed to characterize the development of hippocampal subregion volumes from childhood to adulthood. Second, previous studies of sex differences in hippocampal development have been inconsistent (Herting et al., in press), so we aimed to investigate whether hippocampal subregion volumes and development differs between girls and boys. Finally, we aimed to investigate how hippocampal subregions related to general cognitive ability, which previous studies have found to be related to cortical and white matter structure and development (Shaw et al., 2006; Tamnes et al., 2010; Walhovd et al., 2016).

Materials and Methods

Procedure and participants

The current study was part of the accelerated longitudinal research project *Braintime* (Becht et al., in press; Bos, Peters, van de Kamp, Crone, & Tamnes, under review; Peters & Crone, 2017; Schreuders et al., in press) performed in Leiden, the Netherlands, and approved by the Institutional Review Board at Leiden University Medical Center. Hippocampal subregions have not previously been analyzed in this project. At each time-point (TP), informed consent was obtained from each participant or from a parent in case of minors. Participants received presents and parents received financial reimbursement for travel costs. The participants were recruited through local schools and advertisements across Leiden, The Netherlands. All included participants were required to be fluent in Dutch, right-handed, have normal or corrected-to-normal vision, and to not report neurological or mental health problems or use of psychotropic medication. An initial sample of 299 participants (153 females, 146 males) in the age range 8-26 years old was recruited. All participants were invited to participate in three consecutive waves of data collection approximately two years apart. General cognitive ability was estimated at TP1 and TP2 using different subtests from age-appropriate Wechsler Intelligence Scales (WISC and WAIS) to avoid practice effects; TP1: Similarities and Block Design; TP2: Picture Completion and Vocabulary; TP3: no measurement. All included participants had an estimated IQ ≥ 80.

The final sample for the current study consisted of participants who had at least one structural MRI scan that was successfully processed through both the standard and hippocampal subfield

segmentation longitudinal pipelines of FreeSurfer and which passed our quality control (QC) procedure (see below). This yielded a dataset consisting of 270 participants (145, females, 125 males) with 678 scans (Table 1); 169 participants had scans from 3 TPs, 70 participants had scans from two TPs, and 31 participants had one scan. The mean number of scans per participants was 2.51 (SD = 0.69). The mean interval for longitudinal follow-up scans in the final dataset was 2.11 years (SD = 0.46, range = 1.55-4.43).

[Insert Table 1 about here]

Image acquisition

All scanning was performed on a single 3-Tesla Philips Achieve whole body scanner, using a 6 element SENSE receiver head coil (Philips, Best, The Netherlands) at Leiden University Medical Centre. T1-weighted anatomical scans with the following parameters were obtained at each TP: TR = 9.8 ms, TE = 4.6 ms, flip angel = 8°, 140 slices, 0.875 mm × 0.875 mm × 1.2 mm, and FOV = 224 × 177 × 168 mm. Scan time for this sequence was 4 min 56 s. There were no major scanner hardware or software upgrades during the MRI data collection period. A radiologist reviewed all scans at TP1 and no anomalous findings were reported.

Image analysis

Image processing was performed on the computer network at Leiden University Medical Center. Whole-brain volumetric segmentation and cortical surface reconstruction was performed using FreeSurfer 5.3, a well-validated open-source software suite which is freely available (http://surfer.nmr.mgh.harvard.edu/). The technical details of this automated processing and the specific processing steps are described in detail elsewhere (Dale, Fischl, & Sereno, 1999; Fischl, 2012; Fischl et al., 2002; Fischl, Sereno, & Dale, 1999). Next, the images were processed using FreeSurfer 5.3's longitudinal stream (Reuter, Schmansky, Rosas, & Fischl, 2012). Specifically, an unbiased within-subject template space and image ("base") is created using robust, inverse consistent registration (Reuter, Rosas, & Fischl, 2010). Several processing steps, such as skull stripping, Talairach transforms, atlas registration, and spherical surface maps and parcellations are then initialized with common information from the within-subject template, significantly increasing reliability and statistical power (Reuter et al., 2012).

Detailed post-processing QC in the form of visual inspection focusing both on overall image quality, including motion artifacts, and the accuracy of the whole-brain segmentation and reconstructed

surfaces was then performed on all scans. Scans judged to be of poor quality were excluded and the remaining scans from that participant were reprocessed through the longitudinal pipeline to assure the quality of the within-subject template. This QC procedure was repeated until only acceptable scans were included in the longitudinal processing (note that single time points were also processed longitudinally). No manual editing was performed.

Finally, using FreeSurfer 6.0, the T1-weighthed images were processed using a novel automated algorithm for longitudinal segmentation of hippocampal subregions (Iglesias et al., 2015; Iglesias et al., 2016) (Figure 1). The procedure uses a computational atlas built from high resolution *ex vivo* MRI data, acquired at an average of 0.13 mm isotropic resolution on a 7-Tesla scanner, and an *in vivo* atlas that provides information about adjacent extrahippocampal structures (Iglesias et al., 2015). The unbiased longitudinal segmentation relies on subject-specific atlases and the segmentations at the different TPs are jointly computed using a Bayesian inference algorithm (Iglesias et al., 2016). Compared with the previous algorithm developed by FreeSurfer (Van Leemput et al., 2009), the volumes generated by this new algorithm are more comparable with histologically based measurements of the subfields and much closer to the underlying subregion boundaries (Iglesias et al., 2015). It also provides a more comprehensive, fine-grained segmentation of the structures of the hippocampus. For each hemisphere, the following 12 subregions are segmented: parasubiculum, presubiculum, subiculum, CA1, CA2/3 (combined in the atlas due to indistinguishable MRI contrast), CA4, the granule cell layer of the DG (GC-DG), the molecular layer (ML), fimbria, the hippocampal fissure, the hippocampus-amygdala transition area (HATA), and the hippocampal tail (the posterior end of the hippocampus, which includes portions of the CA fields and DG undistinguishable with the MRI contrast). Test-retest reliability has been found to be high or moderate-to-high for all subregions except the hippocampal fissure in samples of older adults and young adults with T1-weigthed images with standard resolution (Whelan et al., 2016), and to be further improved for nearly all the regions by use of the longitudinal pipeline (Iglesias et al., 2016). In addition to the subregions, a measure of whole hippocampus volume is obtained by adding up the volumes of the subregions (not including the hippocampal fissure). For each scan, volumetric estimates for each annotation was extracted and averaged across hemispheres. Additionally, we extracted measures of estimated intracranial volume (ICV) from an atlas-based spatial normalization procedure (Buckner et al., 2004). Note that as FreeSurfer 5.3's longitudinal pipeline assumes a constant ICV, the ICV measures were extracted from the cross-sectionally processed scans.

[Insert Figure 1 about here]

Statistical analysis

Statistical analyses were performed using IBM SPSS 24.0 (IBM Corporation) and R 3.3.3 (https://www.r-project.org/). To test for reliability over time in our longitudinal sample, intra class correlation (ICC) was calculated for whole hippocampal volume and all subregions (Table 2). Consistent with previous reports (Whelan et al., 2016), ICC was high for all variables except the hippocampal fissure. To investigate developmental trajectories of volume of total hippocampus and each of the 12 hippocampal subregions, and the effects of sex, we used mixed models, performed using the *nlme* package (Pinheiro, Bates, DebRoy, Sarkar, & R Core Team, 2017). Mixed modelling approaches are well suited for accelerated longitudinal designs and able to handle missing data, and for these reasons widely used (Vijayakumar, Mills, Alexander-Bloch, Tamnes, & Whittle, in press). All mixed models followed a formal model-fitting procedure. Preferred models had lower Bayesian Information Criterion (BIC) values. This model selection procedure was used to ensure the most parsimonious model was selected (i.e., choosing the less complex model when the addition of parameters do not improve model fit). First, we ran an unconditional means model including a fixed and random intercept to allow for individual differences. Second, we then compared these models with three often used different growth models (linear, quadratic, and cubic (Casey, 2015)) that tested the grand mean trajectory of age using the polynomial function. Third, we added a random slope to the best fitting age model and tested whether this improved model fit. Fourth, to investigate sex differences in raw volume and volume change over time, we added sex as a main effect and an interaction effect, respectively, to the best fitting model and tested whether either of these improved model fit.

[Insert Table 2 about here]

In a set of follow-up analyses, we added a linear growth model of ICV to the best fitting model and checked how this affected the significance for each of the age terms and sex. However, in our discussion we focus on the results for raw volumes, as we were mainly interested in how subregion volumes change over time, and how these longitudinal developmental patterns are associated with sex and general cognitive ability. First, previous results show that whether and how one includes a global variable like ICV in the statistical analyses may directly influence regional results in complex ways (Dennison et al., 2013; Pintzka, Hansen, Evensmoen, & Håberg, 2015; Sanfilipo, Benedict, Zivadinov, & Bakshi, 2004). Second, recent results also show that global metrics, including ICV, continue to change in late childhood and adolescence (Mills et al., 2016) and controlling for these

measures in developmental studies thus generates a different research question of relative change. Finally, the inclusion of a global variable may be redundant when examining longitudinal change using mixed models, as each subject receives its own intercept and slope (Crone & Elzinga, 2015). Thus, the between-subject variance due to individual differences in head size is captured at the individual level over time; allowing for better characterization of changes in regional volume estimates over time (see also (Herting et al., in press; Vijayakumar et al., in press)).

Finally, we investigated whether level of general cognitive ability could explain variance in hippocampal subregion volumes and/or development. For each participant we calculated an average general cognitive ability score across TP1 and TP2 from the T-scores on the available subtests to obtain a single score per participant. This yielded a subsample of 259 participants with 667 scans (11 participants only had MRI data included from TP3 where no IQ tasks were performed). The mean score for this sample was 109.1 (SD = 9.4, range = 80.0-147.5). We then added this continuous general cognitive ability score (centered) to the best fitting mixed model and checked the significance of its main and age interaction terms. These results were corrected for multiple comparisons using a Bonferroni procedure adjusted for correlated variables (using the mean correlation between the 13 volumes; whole hippocampal volume and the 12 hippocampal subregions) (http://www.quantitativeskills.com/sisa/calculations/bonfer.htm) (Perneger, 1998; Sankoh, Huque, & Dubey, 1997), yielding a significance level for α (2-sided adjusted) = .0144. For visualization only, the sample was split into two approximately equally large subgroups: relatively low (mean = 102.2, SD = 5.5, range = 80.0-108.8, 325 scans) and relatively high (mean = 116.1, SD = 5.5, range = 110.0-147.5, 342 scans) general cognitive ability. Finally, in follow-up analyses for subregions where the general cognitive ability main or age interaction term was significant, we reran the models after adding a linear growth term of ICV.

Results

Hippocampal subregion development

BIC values for the different unconditional means models and age models for the volume of the whole hippocampus and each hippocampal subregion are reported in Table 3. Model parameters for the best fitting models are reported in Table 4. Mixed model analyses on whole hippocampus volume showed a cubic developmental pattern. As shown in Figure 2, whole hippocampus volume increased in late childhood and early adolescence, followed by a slightly decelerating decrease in late adolescence and young adulthood.

[Insert Tables 3 and 4 about here]

[Insert Figure 2 about here]

Best fitting models for all hippocampal subregions are shown in Figure 3. For parasubiculum, presubiculum, CA2/3, CA4 and GC-DG, a linear age model fitted best, with steady volume decreases from late childhood to adulthood. For CA1, a quadratic age model with random slope fitted best, and the quadratic age model was also the best fit for fimbria. For both of these subregion volumes, development followed an inverse-u trajectory. For subiculum and ML volumes, development followed a cubic pattern similar to whole hippocampus volume; early increases, followed by decelerating decreases. Finally, for the three subregions the hippocampal fissure, HATA and the hippocampal tail, the random intercept model fitted better than any of the growth models.

[Insert Figure 3 about here]

Sex effects on hippocampal subregion volumes and development

Both for whole hippocampus volume and for all subregions except the hippocampal fissure, adding sex as a main effect improved model fit (Table 3). In all these regions, boys on average had larger volume than girls (Table 4, Figures 2 and 3). However, adding sex as an interaction effect did not improve model fit for whole hippocampus volume or any of the hippocampal subregions. This indicates parallel developmental trajectories in girls and boys.

ICV adjusted results

In order to better be able to compare our results with some of the previous studies, we added a linear growth model of ICV to the best fitting model for whole hippocampus and each subregion volume (Table 5). ICV was significant for all regions except the hippocampal fissure, while the effect of sex was no longer significant in any region except for whole hippocampus and HATA. For the subregions, most of the age effects remained significant, with the exception of the linear age term for GC-DG and the cubic age term for subiculum and ML.

[Insert Table 5 about here]

General cognitive ability and hippocampal subregion volumes and development

To investigate whether level of general cognitive ability could explain variance in hippocampal volumes and/or development, we added this continuous score as an interaction term to the best

fitting model (Table 6). Significant positive main effects of general cognitive ability were found for two subregions: CA2/3 (B = 0.568, p = .004) and CA4 (B = 0.695, p =.001), such that higher level of performance was related to great volumes. Additionally, there was an uncorrected positive effect for GC-DG (B = 0.513, p =.037). The results also revealed a significant quadratic age × general cognitive ability interaction for ML (B = -6.937, p =.012), and a similar uncorrected effect for subiculum (B = -4.569, p =.042). The results of these analyses with general cognitive ability as a continuous measure are illustrated using subgroups of relatively low and relatively high general cognitive ability (Figure 4). For these subregions where the general cognitive ability main or an age interaction term was significant, we reran the models with a linear growth term of ICV. The positive main effects of general cognitive ability remained significant for CA2/3 (B = 0.459, p = .012) and CA4 (B = 0.552, p =.005), while the previously uncorrected positive effect for GC-DG was no longer significant (B = 0.360, p =.109). After adding a linear trend of ICV, the quadratic age × general cognitive ability interaction showed an uncorrected effect for ML (B = -6.195, p =.028), and was no longer significant for subiculum (B = -3.821, p =.087).

[Insert Table 6 about here]

[Insert Figure 4 about here]

Discussion

The current study of longitudinal development of hippocampal subregions from childhood to adulthood yielded three novel findings. First, the results showed heterogeneous developmental patterns across subregions, with nonlinear trajectories with early volume increases for subiculum, CA1, ML and fimbria, and linear volume decreases or no change in the other subregions. Second, boys showed larger volumes than girls for almost all hippocampal subregions, but boys and girls showed parallel developmental trajectories. Third, general cognitive ability was positively associated with CA2/3 and CA4 volumes and with ML development. These findings will be discussed in more detail in the following paragraphs.

Whole hippocampal volume increased in late childhood and early adolescence, followed by a slightly decelerating decrease in late adolescence and young adulthood, in agreement with accumulating evidence from other studies (Coupe et al., 2017; Herting et al., in press; Narvacan et al., 2017; Wierenga et al., 2014). Most importantly, however, distinct hippocampal subfields showed different developmental trajectories. Subiculum, CA1, ML and fimbria showed nonlinear trajectories with initial volume increases. In stark contrast, parasubiculum, presubiculum, CA2/3, CA4 and GC-DG

showed linear volume decreases. Finally, the hippocampal fissure, HATA and the hippocampal tail showed no development across adolescence.

Our results appear to be consistent with the observed age-related increase in CA1 in the right hemisphere in late childhood and early adolescence in the study by Lee et al., but not with the observed age-related increase in the right CA3/DG in the same study (Lee, Ekstrom, et al., 2014). Compared to the results by Daugherty et al., our results appear consistent with the observed negative age relationship for CA3/DG volume, but partly at odds with the observed negative age relationship for CA1/2 volume (Daugherty et al., 2016). Direct comparisons between our developmental results and previous studies of specific hippocampal subregions (Daugherty et al., 2016; Krogsrud et al., 2014; Lee, Ekstrom, et al., 2014; Tamnes et al., 2014) are however difficult, as the previous studies relied on small and/or cross-sectional samples of children and adolescents. Additionally, two of the previous studies (Daugherty et al., 2016; Lee, Ekstrom, et al., 2014) relied on manual segmentation with its limitations; being laborious and liable to bias and variability (Schlichting, Mack, et al., 2017). Two other previous studies (Krogsrud et al., 2014; Tamnes et al., 2014) used an older automated segmentation procedure which has been found to systemically misestimate specific subregion volumes compared to histological classifications (Schoene-Bake et al., 2014) and for many subregions to show poor agreement with the newer automated procedure used in the present study (Whelan et al., 2016).

We were also interested in testing sex differences in trajectories of hippocampal development. Boys showed larger volumes than girls for all hippocampal subregions except the hippocampal fissure, but adding sex as an interaction term did not improve model fit for any region. Our results therefore do not indicate sexually dimorphic development of hippocampal subregion volumes. Early cross-sectional studies of whole hippocampal volume reported conflicting sex-specific age-related differences (Giedd et al., 1996; Suzuki et al., 2005), but larger or longitudinal studies have not found sexually dimorphic developmental trajectories (Dennison et al., 2013; Koolschijn & Crone, 2013; Wierenga et al., 2014). The present results are also consistent with the previous studies on hippocampal subregions which have found larger absolute volumes in boys (Krogsrud et al., 2014; Tamnes et al., 2014), but no interactions between sex and age (Krogsrud et al., 2014) or sex differences in change rates (Tamnes et al., 2014). Notably, and consistent with several previous reports on sex differences in brain volumes (Marwha, Halari, & Eliot, 2017; Pintzka et al., 2015; Tan, Ma, Vira, Marwha, & Eliot, 2016) and as expected, most of the main effects of sex on hippocampal

subregion volumes disappeared when including ICV in the statistical models, indicating that sex plays a minor role for hippocampal subregion volume differences.

Functionally, it is likely that different parts of the hippocampus have somewhat different roles for different aspects of cognition and behavior. Our results showed that higher general cognitive ability was associated with greater CA2/3 and CA4 volumes across the investigated age-span. Additionally, general cognitive ability was also associated with the developmental trajectory for ML volume, such that individuals with higher scores showed a slightly more nonlinear development. A similar association has previously been found between general intellectual ability and cortical development (Shaw et al., 2006). Previous studies of hippocampal subregion volumes and development in children and adolescents have focused on associations with learning and memory (Daugherty, Flinn, & Ofen, 2017; DeMaster et al., 2014; Lee, Ekstrom, et al., 2014; Riggins, Blankenship, Mulligan, Rice, & Redcay, 2015; Schlichting, Guarino, Schapiro, Turk-Browne, & Preston, 2017; Tamnes et al., 2014). For instance, a recent study found that a multivariate profile of age-related differences in intrahippocampal volumes was associated with differences in encoding of unique memory representations (Keresztes et al., 2017). The hippocampus does however appear to be involved in a broad specter of cognitive functions and behaviors that may also include e.g. spatial navigation, emotional behavior, stress regulation, imagination and prediction (Aribisala et al., 2014; Lee, Johnson, & Ghetti, 2017; Mullally & Maguire, 2014; Rubin, Watson, Duff, & Cohen, 2014). Intriguingly, in a large study of older adults, general intelligence was found to be associated with several measures of tissue microstructure in the hippocampus, which were derived from diffusion tensor imaging, magnetization transfer and relaxometry, but not with whole hippocampus volume (Aribisala et al., 2014). This suggested that more subtle differences in the hippocampus may reflect differences in general cognitive ability, at least in the elderly (see also (Reuben, Brickman, Muraskin, Steffener, & Stern, 2011)). Our results add to this picture by indicating that specific hippocampal subregion volumes and developmental patterns are also be associated with general cognitive ability in youth.

Our study has several strengths such as a longitudinal design, a large sample size, the use of a new hippocampal subregion segmentation tool, and longitudinal image processing; however, there are also some limitations that should be considered. One limitation is that we used only T1-weighthed data acquired on a 3-Tesla scanner with standard resolution (0.875×0.875×1.2 mm). Optimally, scans with higher spatial resolution should be used, and it is also preferable to use a combination of e.g. T1-weighted and T2-weighted data (Iglesias et al., 2015). However, the method employed to

segment hippocampal subregions was developed based on *ex vivo* tissues scanned with ultra-high field strength, and has been demonstrated to be applicable and reliable in datasets with different types of contrast and resolution (Iglesias et al., 2015; Whelan et al., 2016). Nonetheless, results particularly from smaller subregions should be interpreted with caution. A second caveat is that there is disagreement in the literature and across segmentation methods about the placement of certain subfield boundaries, and detailed direct comparisons between the automated method used in the present study and other available methods (Avants et al., 2011; Yushkevich, Amaral, et al., 2015; Yushkevich, Pluta, et al., 2015) are lacking. Importantly, current efforts are however underway to develop a harmonized segmentation protocol (Wisse et al., 2017). Third, we did not investigate longitudinal change in general cognitive ability or more specific cognitive functions. Future studies are needed to further shed light on the functional implications of longitudinal changes in hippocampal subregions, both in terms of development of cognitive functions, and the emergence of mental disorder such as psychosis and depression during adolescence. Finally, we also note that our conclusions from group-level inferences may not translate to individual development, and that appropriate disambiguation of between- and within-person effects in analyses is an issue that deserves more attention in the developmental cognitive neuroscience field (Telzer et al., under review).

Future studies should investigate puberty and hormone effects on development of hippocampal subregion volumes, as it has been found that age and pubertal development have both independent and interactive influences on hippocampus volume change over adolescence (Goddings et al., 2014; Satterthwaite et al., 2014). Further, a recent study showed greater variance in males than females for several brain volumes including the hippocampus (Wierenga et al., in press), and future studies should investigate whether such variability differences are general or specific for distinct hippocampal subregion volumes and development. Next, future developmental studies should integrate subregion segmentation in the transverse plane and along the longitudinal axis of the hippocampus (Lee et al., 2017). Finally, future studies could also investigate development of hippocampal-cortical networks at the level of specific hippocampal subregions, e.g. by analyzing structural covariance (Walhovd et al., 2015), structural connectivity inferred from diffusion MRI (Wendelken et al., 2015), or functional connectivity from functional MRI (Blankenship, Redcay, Dougherty, & Riggins, 2017; Paz-Alonso, Gallego, & Ghetti, 2013).

In conclusion, our results show that hippocampal subregions develop in diversified ways across adolescence, with nonlinear trajectories with early volume increases for subiculum, CA1, ML and

fimbria, and linear volume decreases for parasubiculum, presubiculum, CA2/3, CA4 and GC-DG. Further, while boys had larger hippocampal subregion volumes than girls, there were no sex differences in the development of the subregions. The results also showed that volume and developmental pattern of specific hippocampal subregions was associated with general cognitive ability. However, future replication studies with high-resolution scans are called for. The findings inform future research on the neuroanatomical basis of memory development, and should also be taken into account in studies of brain development in mental disorders including psychosis and depression.

References

Amaral, D., & Lavenex, P. (2007). Hippocampal neuroanatomy. In P. Anderson, R. Morris, D. G. Amaral, T. Bliss, & J. O'Keefe (Eds.), *The Hippocampus Book* (pp. 37-114). New York: Oxford UP.

Aribisala, B. S., Royle, N. A., Maniega, S. M., Valdes Hernandez, M. C., Murray, C., Penke, L., . . . Wardlaw, J. M. (2014). Quantitative multi-modal MRI of the Hippocampus and cognitive ability in community-dwelling older subjects. *Cortex, 53*, 34-44.

Avants, B. B., Tustison, N. J., Song, G., Cook, P. A., Klein, A., & Gee, J. C. (2011). A reproducible evaluation of ANTs similarity metric performance in brain image registration. *Neuroimage, 54*, 2033-2044.

Becht, A. I., Bos, M. G. N., Nelemans, S. A., Peters, S., Vollebergh, W. A. M., Branje, S. J. T., . . . Crone, E. A. (in press). Goal-directed correlates and neurobiological underpinnings of adolescent identity: A multi-method multi-sample longitudinal approach. *Child Dev*.

Blankenship, S. L., Redcay, E., Dougherty, L. R., & Riggins, T. (2017). Development of hippocampal functional connectivity during childhood. *Hum Brain Mapp, 38*, 182-201.

Bos, M. G. N., Peters, S., van de Kamp, F. C., Crone, E. A., & Tamnes, C. K. (under review). Emerging depression in adolescence coincides with accelerated cortical thinning.

Brown, T. T., Kuperman, J. M., Chung, Y., Erhart, M., McCabe, C., Hagler, D. J., Jr., . . . Dale, A. M. (2012). Neuroanatomical assessment of biological maturity. *Curr Biol, 22*, 1693-1698.

Buckner, R. L., Head, D., Parker, J., Fotenos, A. F., Marcus, D., Morris, J. C., & Snyder, A. Z. (2004). A unified approach for morphometric and functional data analysis in young, old, and demented adults using automated atlas-based head size normalization: reliability and validation against manual measurement of total intracranial volume. *Neuroimage, 23*, 724-738.

Button, K. S., Ioannidis, J. P., Mokrysz, C., Nosek, B. A., Flint, J., Robinson, E. S., & Munafo, M. R. (2013). Power failure: why small sample size undermines the reliability of neuroscience. *Nat Rev Neurosci, 14*, 365-376.

Casey, B. J. (2015). Beyond simple models of self-control to circuit-based accounts of adolescent behavior. *Annu Rev Psychol, 66*, 295-319.

Coupe, P., Catheline, G., Lanuza, E., Manjon, J. V., & Alzheimer's Disease Neuroimaging Initiative. (2017). Towards a unified analysis of brain maturation and aging across the entire lifespan: A MRI analysis. *Hum Brain Mapp, 38*, 5501-5518.

Crone, E. A., & Elzinga, B. M. (2015). Changing brains: how longitudinal functional magnetic resonance imaging studies can inform us about cognitive and social-affective growth trajectories. *Wiley Interdiscip Rev Cogn Sci, 6*, 53-63.

Dale, A. M., Fischl, B., & Sereno, M. I. (1999). Cortical surface-based analysis. I. Segmentation and surface reconstruction. *Neuroimage, 9*, 179-194.

Daugherty, A. M., Bender, A. R., Raz, N., & Ofen, N. (2016). Age differences in hippocampal subfield volumes from childhood to late adulthood. *Hippocampus, 26*, 220-228.

Daugherty, A. M., Flinn, R., & Ofen, N. (2017). Hippocampal CA3-dentate gyrus volume uniquely linked to improvement in associative memory from childhood to adulthood. *Neuroimage, 153*, 75-85.

de Flores, R., La Joie, R., Landeau, B., Perrotin, A., Mezenge, F., de La Sayette, V., . . . Chetelat, G. (2015). Effects of age and Alzheimer's disease on hippocampal subfields: comparison between manual and FreeSurfer volumetry. *Hum Brain Mapp, 36*, 463-474.

DeMaster, D., Pathman, T., Lee, J. K., & Ghetti, S. (2014). Structural development of the hippocampus and episodic memory: developmental differences along the anterior/posterior axis. *Cereb Cortex, 24*, 3036-3045.

Dennison, M., Whittle, S., Yucel, M., Vijayakumar, N., Kline, A., Simmons, J., & Allen, N. B. (2013). Mapping subcortical brain maturation during adolescence: evidence of hemisphere- and sex-specific longitudinal changes. *Dev Sci, 16*, 772-791.

Ekstrom, A. D., Bazih, A. J., Suthana, N. A., Al-Hakim, R., Ogura, K., Zeineh, M., . . . Bookheimer, S. Y. (2009). Advances in high-resolution imaging and computational unfolding of the human hippocampus. *Neuroimage, 47*, 42-49.

Fischl, B. (2012). FreeSurfer. *Neuroimage, 62*, 774-781.

Fischl, B., Salat, D. H., Busa, E., Albert, M., Dieterich, M., Haselgrove, C., . . . Dale, A. M. (2002). Whole brain segmentation: automated labeling of neuroanatomical structures in the human brain. *Neuron, 33*, 341-355.

Fischl, B., Sereno, M. I., & Dale, A. M. (1999). Cortical surface-based analysis. II: Inflation, flattening, and a surface-based coordinate system. *Neuroimage, 9*, 195-207.

Ghetti, S., & Bunge, S. A. (2012). Neural changes underlying the development of episodic memory during middle childhood. *Dev Cogn Neurosci, 2*, 381-395.

Giedd, J. N., Vaituzis, A., Hamburger, S. D., Lange, N., Rajapakse, J. C., Kaysen, D., . . . Rapoport, J. L. (1996). Quantitative MRI of the temporal lobe, amygdala, and hippocampus in normal human development: Ages 4-18 years. *J Comp Neurol, 366*, 223-230.

Gilmore, J. H., Shi, F., Woolson, S. L., Knickmeyer, R. C., Short, S. J., Lin, W., . . . Shen, D. (2012). Longitudinal development of cortical and subcortical gray matter from birth to 2 years. *Cereb Cortex, 22*, 2478-2485.

Goddings, A. L., Mills, K. L., Clasen, L. S., Giedd, J. N., Viner, R. M., & Blakemore, S. J. (2014). The influence of puberty on subcortical brain development. *Neuroimage, 88*, 242-251.

Gogtay, N., Nugent, T. F., Herman, D. H., Ordonez, A., Greenstein, D., Hayashi, K. M., . . . Thompson, P. M. (2006). Dynamic mapping of normal human hippocampal development. *Hippocampus, 16*, 664-672.

Herting, M. M., Johnson, C., Mills, K. L., Vijayakumar, N., Dennison, M., Liu, C., . . . Tamnes, C. K. (in press). Development of subcortical volumes across adolescence in males and females: A multisample study of longitudinal changes. *Neuroimage*.

Hu, S., Pruessner, J. C., Coupe, P., & Collins, D. L. (2013). Volumetric analysis of medial temporal lobe structures in brain development from childhood to adolescence. *Neuroimage, 74*, 276-287.

Iglesias, J. E., Augustinack, J. C., Nguyen, K., Player, C. M., Player, A., Wright, M., . . . Alzheimer's Disease Neuroimaging Initiative. (2015). A computational atlas of the hippocampal formation using ex vivo, ultra-high resolution MRI: Application to adaptive segmentation of in vivo MRI. *Neuroimage, 115*, 117-137.

Iglesias, J. E., Van Leemput, K., Augustinack, J., Insausti, R., Fischl, B., Reuter, M., & Alzheimer's Disease Neuroimaging Initiative. (2016). Bayesian longitudinal segmentation of hippocampal substructures in brain MRI using subject-specific atlases. *Neuroimage, 141*, 542-555.

Insausti, R., & Amaral, D. G. (2012). Hippocampal formation. In J. K. Mai & G. Paxinos (Eds.), *The Human Nervous System* (pp. 896-942). Amsterdam: Elsevier Inc.

Insausti, R., Cebada-Sanchez, S., & Marcos, P. (2010). Postnatal development of the human hippocampal formation. *Adv Anat Embryol Cell Biol, 206*, 1-86.

Keresztes, A., Bender, A. R., Bodammer, N. C., Lindenberger, U., Shing, Y. L., & Werkle-Bergner, M. (2017). Hippocampal maturity promotes memory distinctiveness in childhood and adolescence. *Proc Natl Acad Sci U S A, 114*, 9212-9217.

Koolschijn, P. C., & Crone, E. A. (2013). Sex differences and structural brain maturation from childhood to early adulthood. *Dev Cogn Neurosci, 5*, 106-118.

Krogsrud, S. K., Tamnes, C. K., Fjell, A. M., Amlien, I., Grydeland, H., Sulutvedt, U., . . . Walhovd, K. B. (2014). Development of hippocampal subfield volumes from 4 to 22 years. *Hum Brain Mapp, 35*, 5646-5657.

Lee, F. S., Heimer, H., Giedd, J. N., Lein, E. S., Sestan, N., Weinberger, D. R., & Casey, B. J. (2014). Mental health. Adolescent mental health--opportunity and obligation. *Science, 346*, 547-549.

Lee, J. K., Ekstrom, A. D., & Ghetti, S. (2014). Volume of hippocampal subfields and episodic memory in childhood and adolescence. *Neuroimage, 94*, 162-171.

Lee, J. K., Johnson, E. G., & Ghetti, S. (2017). Hippocampal development: Structure, function and implications. In D. E. Hannula & M. C. Duff (Eds.), *The hippocampus from cells to systems: Structure, connectivity, and functional contributions to memory and flexible cognition* (pp. 141-166): Springer International Publishing AG.

Marwha, D., Halari, M., & Eliot, L. (2017). Meta-analysis reveals a lack of sexual dimorphism in human amygdala volume. *Neuroimage, 147*, 282-294.

Mattai, A., Hosanagar, A., Weisinger, B., Greenstein, D., Stidd, R., Clasen, L., . . . Gogtay, N. (2011). Hippocampal volume development in healthy siblings of childhood-onset schizophrenia patients. *Am J Psychiatry, 168*, 427-435.

Mills, K. L., Goddings, A. L., Herting, M. M., Meuwese, R., Blakemore, S. J., Crone, E. A., . . . Tamnes, C. K. (2016). Structural brain development between childhood and adulthood: Convergence across four longitudinal samples. *Neuroimage, 141*, 273-281.

Mueller, S. G., Stables, L., Du, A. T., Schuff, N., Truran, D., Cashdollar, N., & Weiner, M. W. (2007). Measurement of hippocampal subfields and age-related changes with high resolution MRI at 4T. *Neurobiol Aging, 28*, 719-726.

Muftuler, L. T., Davis, E. P., Buss, C., Head, K., Hasso, A. N., & Sandman, C. A. (2011). Cortical and subcortical changes in typically developing preadolescent children. *Brain Res, 1399*, 15-24.

Mullally, S. L., & Maguire, E. A. (2014). Memory, Imagination, and Predicting the Future: A Common Brain Mechanism? *Neuroscientist, 20*, 220-234.

Narvacan, K., Treit, S., Camicioli, R., Martin, W., & Beaulieu, C. (2017). Evolution of deep gray matter volume across the human lifespan. *Hum Brain Mapp, 38*, 3771-3790.

Nord, C. L., Valton, V., Wood, J., & Roiser, J. P. (2017). Power-up: a reanalysis of 'power failure' in neuroscience using mixture modelling. *J Neurosci, 37*, 8051-8061.

Open Science Collaboration. (2015). Estimating the reproducibility of psychological science. *Science, 349*, aac4716.

Paz-Alonso, P. M., Gallego, P., & Ghetti, S. (2013). Age differences in hippocampus-cortex connectivity during true and false memory retrieval. *J Int Neuropsychol Soc, 19*, 1031-1041.

Perneger, T. V. (1998). What's wrong with Bonferroni adjustments. *BMJ, 316*, 1236-1238.

Peters, S., & Crone, E. A. (2017). Increased striatal activity in adolescence benefits learning. *Nat Commun, 8*, 1983.

Pinheiro, J., Bates, D., DebRoy, S., Sarkar, D., & R Core Team. (2017). nlme: Linear and nonlinear mixed effects models. R package version 3.1-131. *https://CRAN.R-project.org/package=nlme*.

Pintzka, C. W., Hansen, T. I., Evensmoen, H. R., & Håberg, A. K. (2015). Marked effects of intracranial volume correction methods on sex differences in neuroanatomical structures: a HUNT MRI study. *Front Neurosci, 9*, 238.

Reuben, A., Brickman, A. M., Muraskin, J., Steffener, J., & Stern, Y. (2011). Hippocampal atrophy relates to fluid intelligence decline in the elderly. *J Int Neuropsychol Soc, 17*, 56-61.

Reuter, M., Rosas, H. D., & Fischl, B. (2010). Highly accurate inverse consistent registration: a robust approach. *Neuroimage, 53*, 1181-1196.

Reuter, M., Schmansky, N. J., Rosas, H. D., & Fischl, B. (2012). Within-subject template estimation for unbiased longitudinal image analysis. *Neuroimage, 61*, 1402-1418.

Riggins, T., Blankenship, S. L., Mulligan, E., Rice, K., & Redcay, E. (2015). Developmental differences in relations between episodic memory and hippocampal subregion volume during early childhood. *Child Dev, 86*, 1710-1718.

Rubin, R. D., Watson, P. D., Duff, M. C., & Cohen, N. J. (2014). The role of the hippocampus in flexible cognition and social behavior. *Front Hum Neurosci, 8*, 742.

Sanfilipo, M. P., Benedict, R. H., Zivadinov, R., & Bakshi, R. (2004). Correction for intracranial volume in analysis of whole brain atrophy in multiple sclerosis: the proportion vs. residual method. *Neuroimage, 22*, 1732-1743.

Sankoh, A. J., Huque, M. F., & Dubey, S. D. (1997). Some comments on frequently used multiple endpoint adjustment methods in clinical trials. *Stat Med, 16*, 2529-2542.

Satterthwaite, T. D., Vandekar, S., Wolf, D. H., Ruparel, K., Roalf, D. R., Jackson, C., . . . Gur, R. C. (2014). Sex differences in the effect of puberty on hippocampal morphology. *J Am Acad Child Adolesc Psychiatry, 53*, 341-350 e341.

Schlichting, M. L., Guarino, K. F., Schapiro, A. C., Turk-Browne, N. B., & Preston, A. R. (2017). Hippocampal structure predicts statistical learning and associative inference abilities during development. *J Cogn Neurosci, 29*, 37-51.

Schlichting, M. L., Mack, M. L., Guarine, K. F., & Preston, A. R. (2017). Comparison of semi-automated hippocampal subfield segmentation methods in a pediatric sample. *bioRxiv, 064303*.

Schmaal, L., Veltman, D. J., van Erp, T. G., Samann, P. G., Frodl, T., Jahanshad, N., . . . Hibar, D. P. (2016). Subcortical brain alterations in major depressive disorder: findings from the ENIGMA Major Depressive Disorder working group. *Mol Psychiatry, 21*, 806-812.

Schoene-Bake, J. C., Keller, S. S., Niehusmann, P., Volmering, E., Elger, C., Deppe, M., & Weber, B. (2014). In vivo mapping of hippocampal subfields in mesial temporal lobe epilepsy: relation to histopathology. *Hum Brain Mapp, 35*, 4718-4728.

Schreuders, E., Braams, B. R., Blakenstein, N. E., Peper, J. S., Güroğlu, B., & Crone, E. A. (in press). Contributions of reward sensitivity to ventral striatum activity across adolescence and early adulthood. *Child Dev*.

Shaw, P., Greenstein, D., Lerch, J., Clasen, L., Lenroot, R., Gogtay, N., . . . Giedd, J. (2006). Intellectual ability and cortical development in children and adolescents. *Nature, 440*, 676-679.

Sullivan, E. V., Pfefferbaum, A., Rohlfing, T., Baker, F. C., Padilla, M. L., & Colrain, I. M. (2011). Developmental change in regional brain structure over 7 months in early adolescence: comparison of approaches for longitudinal atlas-based parcellation. *Neuroimage, 57*, 214-224.

Suzuki, M., Hagino, H., Nohara, S., Zhou, S. Y., Kawasaki, Y., Takahashi, T., . . . Kurachi, M. (2005). Male-specific volume expansion of the human hippocampus during adolescence. *Cereb Cortex, 15*, 187-193.

Swagerman, S. C., Brouwer, R. M., de Geus, E. J., Hulshoff Pol, H. E., & Boomsma, D. I. (2014). Development and heritability of subcortical brain volumes at ages 9 and 12. *Genes Brain Behav, 13*, 733-742.

Tamnes, C. K., Walhovd, K. B., Dale, A. M., Østby, Y., Grydeland, H., Richardson, G., . . . Alzheimer's Disease Neuroimaging Initiative. (2013). Brain development and aging: overlapping and unique patterns of change. *Neuroimage, 68*, 63-74.

Tamnes, C. K., Walhovd, K. B., Engvig, A., Grydeland, H., Krogsrud, S. K., Østby, Y., . . . Fjell, A. M. (2014). Regional hippocampal volumes and development predict learning and memory. *Dev Neurosci, 36*, 161-174.

Tamnes, C. K., Østby, Y., Walhovd, K. B., Westlye, L. T., Due-Tønnessen, P., & Fjell, A. M. (2010). Intellectual abilities and white matter microstructure in development: a diffusion tensor imaging study. *Hum Brain Mapp, 31*, 1609-1625.

Tan, A., Ma, W., Vira, A., Marwha, D., & Eliot, L. (2016). The human hippocampus is not sexually-dimorphic: Meta-analysis of structural MRI volumes. *Neuroimage, 124*, 350-366.

Telzer, E. H., McCormick, E. M., Peters, S., Cosme, D., Pfeifer, J. H., & van Duijvenvoorde, A. C. (under review). Methodological considerations for developmental longitudinal fMRI research.

Uematsu, A., Matsui, M., Tanaka, C., Takahashi, T., Noguchi, K., Suzuki, M., & Nishijo, H. (2012). Developmental trajectories of amygdala and hippocampus from infancy to early adulthood in healthy individuals. *PLoS One, 7*, e46970.

van Erp, T. G., Hibar, D. P., Rasmussen, J. M., Glahn, D. C., Pearlson, G. D., Andreassen, O. A., . . . Turner, J. A. (2016). Subcortical brain volume abnormalities in 2028 individuals with schizophrenia and 2540 healthy controls via the ENIGMA consortium. *Mol Psychiatry, 21*, 547-553.

Van Leemput, K., Bakkour, A., Benner, T., Wiggins, G., Wald, L. L., Augustinack, J., . . . Fischl, B. (2009). Automated segmentation of hippocampal subfields from ultra-high resolution in vivo MRI. *Hippocampus, 19*, 549-557.

Vijayakumar, N., Mills, K. L., Alexander-Bloch, A., Tamnes, C. K., & Whittle, S. (in press). Structural brain development: a review of methodological approaches and best practices. *Dev Cogn Neurosci*.

Walhovd, K. B., Krogsrud, S. K., Amlien, I. K., Bartsch, H., Bjørnerud, A., Due-Tønnessen, P., . . . Fjell, A. M. (2016). Neurodevelopmental origins of lifespan changes in brain and cognition. *Proc Natl Acad Sci U S A, 113*, 9357-9362.

Walhovd, K. B., Tamnes, C. K., Bjørnerud, A., Due-Tønnessen, P., Holland, D., Dale, A. M., & Fjell, A. M. (2015). Maturation of cortico-subcortical structural networks - Segregation and overlap of medial temporal and fronto-striatal systems in development. *Cereb Cortex, 25*, 1835-1841.

Wendelken, C., Lee, J. K., Pospisil, J., Sastre, M., 3rd, Ross, J. M., Bunge, S. A., & Ghetti, S. (2015). White Matter Tracts Connected to the Medial Temporal Lobe Support the Development of Mnemonic Control. *Cereb Cortex, 25*, 2574-2583.

Whelan, C. D., Hibar, D. P., van Velzen, L. S., Zannas, A. S., Carrillo-Roa, T., McMahon, K., . . . Alzheimer's Disease Neuroimaging Initiative. (2016). Heritability and reliability of automatically segmented human hippocampal formation subregions. *Neuroimage, 128*, 125-137.

Whiteford, H. A., Degenhardt, L., Rehm, J., Baxter, A. J., Ferrari, A. J., Erskine, H. E., . . . Vos, T. (2013). Global burden of disease attributable to mental and substance use disorders: findings from the Global Burden of Disease Study 2010. *Lancet, 382*, 1575-1586.

Wierenga, L. M., Langen, M., Ambrosino, S., van Dijk, S., Oranje, B., & Durston, S. (2014). Typical development of basal ganglia, hippocampus, amygdala and cerebellum from age 7 to 24. *Neuroimage, 96*, 67-72.

Wierenga, L. M., Sexton, J. A., Laake, P., Giedd, J. N., Tamnes, C. K., & the Pediatric Imaging Neurocognition and Genetics Study. (in press). A key characteristic of sex differences in the developing brain: Greater variability in brain structure of boys than girls. *Cereb Cortex*.

Wisse, L. E., Biessels, G. J., & Geerlings, M. I. (2014). A critical appraisal of the hippocampal subfield segmentation package in freeSurfer. *Front Aging Neurosci, 6*, 261.

Wisse, L. E. M., Daugherty, A. M., Olsen, R. K., Berron, D., Carr, V. A., Stark, C. E. L., . . . Hippocampal Subfields Group. (2017). A harmonized segmentation protocol for hippocampal and parahippocampal subregions: Why do we need one and what are the key goals? *Hippocampus, 27*, 3-11.

Yurgelun-Todd, D. A., Killgore, W. D., & Cintron, C. B. (2003). Cognitive correlates of medial temporal lobe development across adolescence: a magnetic resonance imaging study. *Percept Mot Skills, 96*, 3-17.

Yushkevich, P. A., Amaral, R. S., Augustinack, J. C., Bender, A. R., Bernstein, J. D., Boccardi, M., . . . Hippocampal Subfields Group. (2015). Quantitative comparison of 21 protocols for labeling hippocampal subfields and parahippocampal subregions in in vivo MRI: towards a harmonized segmentation protocol. *Neuroimage, 111*, 526-541.

Yushkevich, P. A., Pluta, J. B., Wang, H., Xie, L., Ding, S. L., Gertje, E. C., . . . Wolk, D. A. (2015). Automated volumetry and regional thickness analysis of hippocampal subfields and medial temporal cortical structures in mild cognitive impairment. *Hum Brain Mapp, 36*, 258-287.

Østby, Y., Tamnes, C. K., Fjell, A. M., & Walhovd, K. B. (2012). Dissociating memory processes in the developing brain: the role of hippocampal volume and cortical thickness in recall after minutes versus days. *Cereb Cortex, 22*, 381-390.

Østby, Y., Tamnes, C. K., Fjell, A. M., Westlye, L. T., Due-Tønnessen, P., & Walhovd, K. B. (2009). Heterogeneity in subcortical brain development: A structural magnetic resonance imaging study of brain maturation from 8 to 30 years. *J Neurosci, 29*, 11772-11782.

Figures

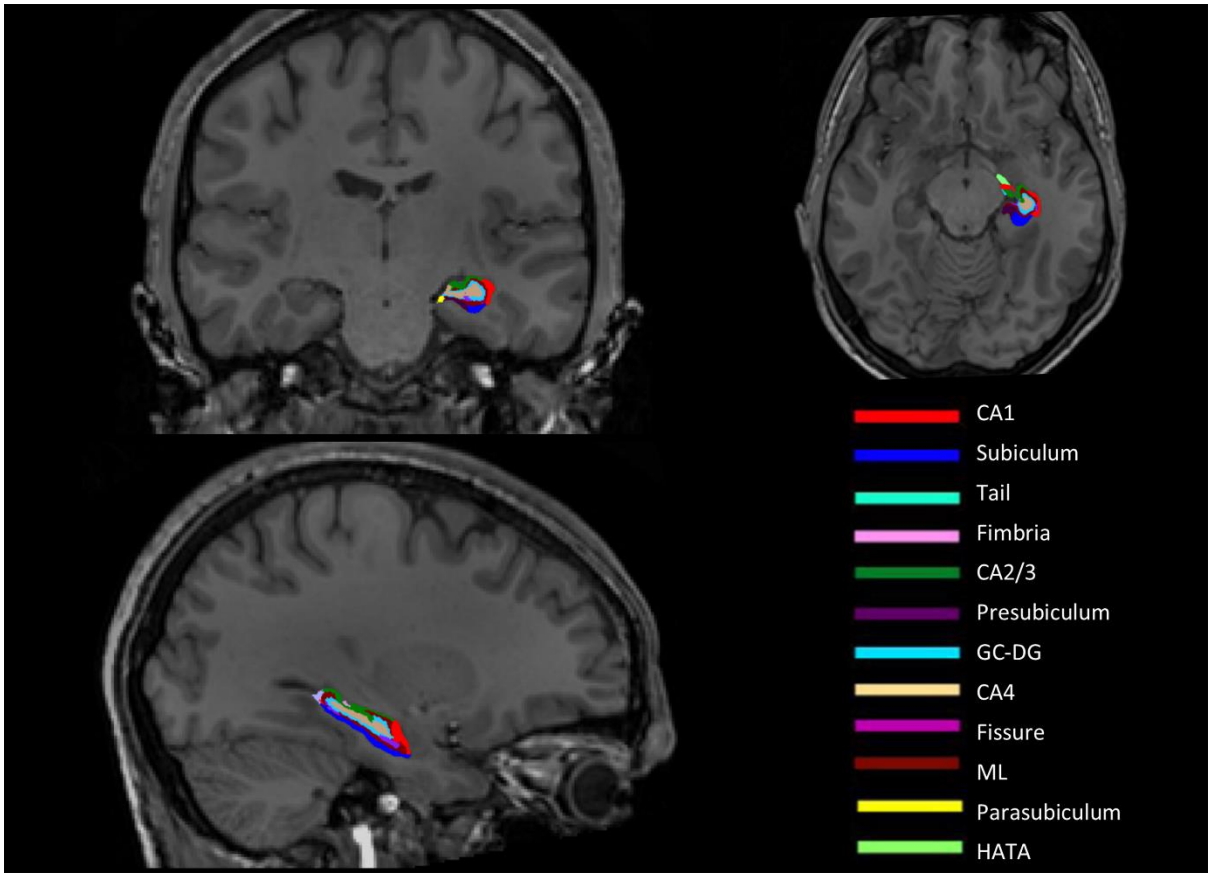

Figure 1. Color-coded illustration of the hippocampal subregions in coronal (top left), horizontal (top right) and sagittal (bottom left) views from a representative participant. The subregion volumes are overlaid on the whole-brain T1-weighted longitudinally processed image.

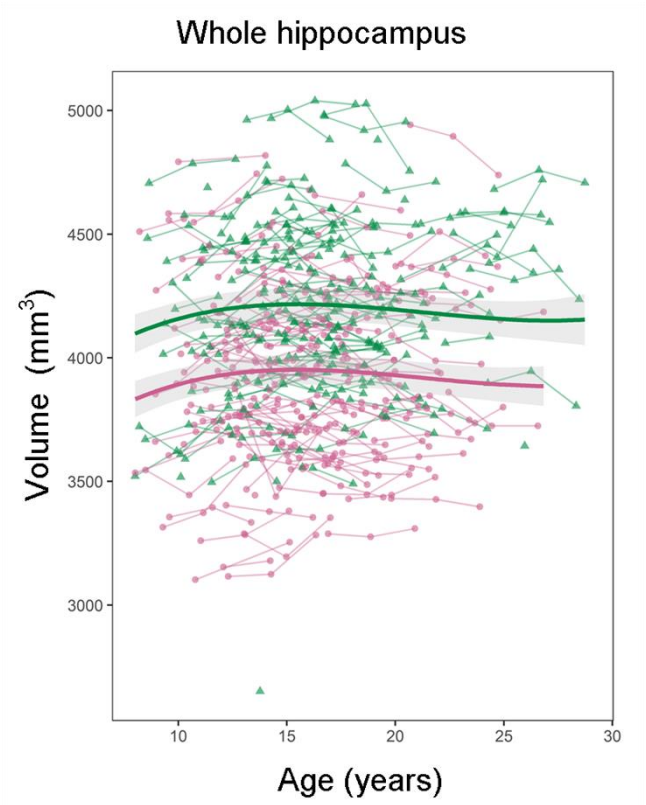

Figure 2. Development of whole hippocampus volume. Volume (y-axis) by age (x-axis) and the optimal fitting model, a cubic model, is shown. The shaded areas represents the 95% confidence intervals. Individual boys (green) and girls (pink) are represented by individual lines, and participants measured once are represented by dots.

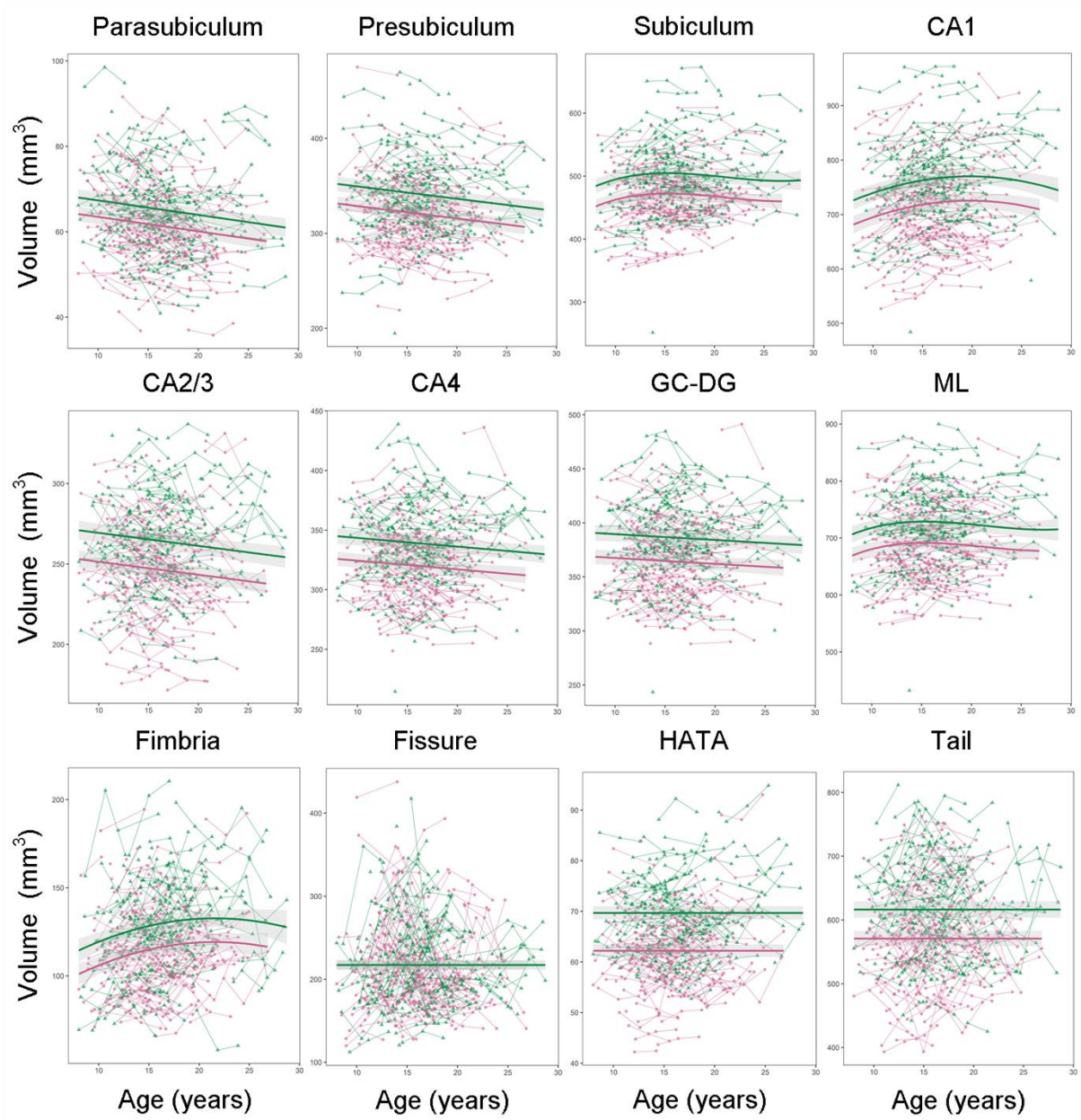

Figure 3. Development of hippocampal subregions. Volumes (y-axis) by age (x-axis) and the optimal fitting models are shown. A linear model fitted best for parasubiculum, presubiculum, CA2/3, CA4 and GC-DG, a quadratic model fitted best for CA1 and fimbria, a cubic model fitted best for subiculum and ML, and a random intercept model fitted best for the hippocampal fissure, HATA and the hippocampal tail. The shaded areas represents the 95% confidence intervals. Individual boys (green) and girls (pink) are represented by individual lines, and participants measured once are represented by dots.

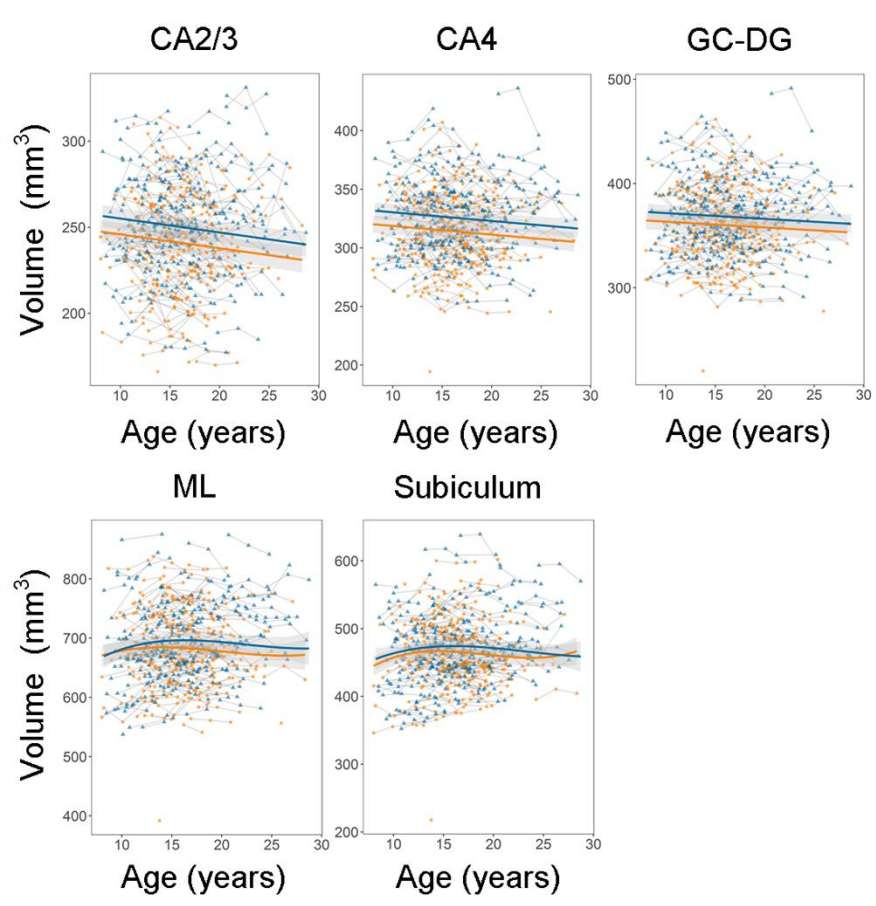

Figure 4. Associations between general cognitive ability and hippocampal subregion volumes and development. For visualization purposes, the sample was split into two groups: relatively high (blue) and relatively low (orange) general cognitive ability. Note that the statistical analyses were performed using a continuous general cognitive ability score, and by adding this score as an interaction term to the best fitting model. Volumes (y-axis) by age (x-axis) are shown and the shaded areas represents the 95% confidence intervals.

Tables

Table 1. Sample characteristics for each time-point (TP)

	TP1	TP2	TP3
n	237	224	217
n females/males	128/109	118/106	119/98
Age, mean (SD)	14.5 (3.7)	16.4 (3.6)	18.4 (3.7)
Age, range	8.0 – 26.0	9.9 – 26.6	11.9 – 28.7
Estimated IQ, mean (SD)	110.0 (10.2)	108.5 (10.1)[a]	–
Estimated IQ, range	80 – 138	80 – 148[a]	–

[a] data missing for 1 participant

Table 2. Intra class correlation (ICC) for whole hippocampus and hippocampal subregion volumes

Region	**ICC**
Whole hippocampus	0.969
Parasubiculum	0.937
Presubiculum	0.953
Subiculum	0.962
CA1	0.966
CA2/3	0.948
CA4	0.944
GC-DG	0.951
ML	0.965
Fimbria	0.867
Hippocampal fissure	0.694
HATA	0.918
Hippocampal tail	0.866

Notes. CA = cornu ammonis, GC-DG = granule cell layer of dentate gyrus, ML = molecular layer, HATA = hippocampus-amygdala transition area.

Table 3. BIC values for the comparison of different mixed models examining age and sex effect on whole hippocampus and hippocampal subregion volumes

Region	**Intercept only**	**Random intercept**	**Age: Linear**	**Age: Quadratic**	**Age: Cubic**	**Random slope**	**Sex main effect**	**Sex interaction effect**
Whole hippocampus	9998	8838	8845	8833	**8831**	8839	**8804**	8818
Parasubiculum	5061	4170	**4143**	4149	4155	4154	**4139**	4145
Presubiculum	6966	5984	**5953**	5958	5960	5966	**5942**	5946
Subiculum	7362	6291	6298	6282	**6277**	6277	**6260**	6273
CA1	7970	6845	6822	**6788**	6791	**6787**	**6774**	6779
CA2/3	6605	5643	**5627**	5633	5639	5639	**5610**	5613
CA4	6723	5801	**5794**	5800	5803	5802	**5779**	5784
GC-DG	6883	5907	**5906**	5912	5913	5914	**5890**	5895
ML	7687	6585	6592	6580	**6578**	6587	**6565**	6579
Fimbria	6397	5796	5780	**5776**	5779	5789	**5764**	5776
Hippocampal fissure	7310	**7031**	7038	7041	7043	7042	7037	-
HATA	4852	**4062**	4064	4069	4075	4071	**4009**	-
Hippocampal tail	7877	**7272**	7274	7279	7285	7285	**7254**	-

Notes. CA = cornu ammonis, GC-DG = granule cell layer of dentate gyrus, ML = molecular layer, HATA = hippocampus-amygdala transition area. Bold indicate the best model for each of the following steps: 1) unconditional means and growth models, 2) best model with random slope model, and 3) best model with sex effects.

Table 4. Model parameters for fixed effects in the best fitting model for whole hippocampus and hippocampal subregion volumes

Region	**B**	**P**	**95% CI, lower**	**95% CI, upper**
Whole hippocampus				
Intercept	3933.064	**<.001**	3873.702	3992.427
Age	-66.854	.689	-393.490	259.782
Age^2	-505.641	**<.001**	-737.577	-273.705
Age^3	251.219	**.006**	74.760	427.677
Sex	265.136	**<.001**	178.115	352.157
Parasubiculum				
Intercept	61.334	**<.001**	59.760	62.909
Age	-35.264	**<.001**	-46.787	-23.742
Sex	3.854	**.001**	1.546	6.162
Presubiculum				
Intercept	320.473	**<.001**	313.881	327.064
Age	-135.035	**<.001**	-176.518	-93.552
Sex	20.670	**<.001**	11.009	30.331
Subiculum				
Intercept	469.020	**<.001**	460.364	477.676
Age	-23.043	.380	-74.420	28.335
Age^2	-87.724	**<.001**	-124.339	-51.109
Age^3	47.468	**<.001**	19.565	75.372
Sex	32.278	**<.001**	19.589	44.966
CA1				
Intercept	716.745	**<.001**	703.216	730.274
Age	164.180	**<.001**	82.712	245.648
Age^2	-175.254	**<.001**	-232.447	-118.060
Sex	44.658	**<.001**	24.860	64.456
CA2/3				
Intercept	246.277	**<.001**	241.339	251.215
Age	-83.865	**<.001**	-117.065	-50.666
Sex	17.946	**<.001**	10.709	25.184
CA4				

Intercept	319.765	**<.001**	314.345	325.285
Age	-75.888	**<.001**	-114.028	-37.749
Sex	19.089	**<.001**	11.145	27.032
GC-DG				
Intercept	364.080	**<.001**	358.011	370.149
Age	-56.327	**.007**	-97.123	-15.530
Sex	22.088	**<.001**	13.193	30.983
ML				
Intercept	687.762	**<.001**	676.565	698.869
Age	-24.230	.456	-87.772	39.311
Age^2	-98.795	**<.001**	-143.996	-53.595
Age^3	49.098	**.006**	14.682	83.515
Sex	37.257	**<.001**	20.976	53.538
Fimbria				
Intercept	114.978	**<.001**	110.915	119.041
Age	88.412	**<.001**	46.426	130.397
Age^2	-54.359	**<.001**	-85.994	-22.724
Sex	13.428	**<.001**	7.475	19.382
Hippocampal fissure				
Intercept	217.245	**<.001**	211.468	223.023
HATA				
Intercept	62.231	**<.001**	61.002	63.461
Sex	7.467	**<.001**	5.664	9.270
Hippocampal tail				
Intercept	570.863	**<.001**	558.888	582.838
Sex	45.396	**<.001**	27.836	62.956

Notes. CI = confidence interval. Bold indicates $p < .05$.

Table 5. Model parameters for fixed effects when including a linear growth model of ICV in the best fitting models for whole hippocampus and hippocampal subregion volumes

Region	**B**	**P**
Whole hippocampus		
Intercept	4002.626	**<.001**
Age	289.818	.093
Age^2	-227.507	.068
Age^3	123.706	.185
Sex	115.089	**.006**
ICV	3256.565	**<.001**
Parasubiculum		
Intercept	62.147	**<.001**
Age	-32.475	**<.001**
Sex	2.090	.099
ICV	38.415	**.001**
Presubiculum		
Intercept	326.265	**<.001**
Age	-112.343	**<.001**
Sex	8.124	.107
ICV	272.919	**<.001**
Subiculum		
Intercept	479.746	**<.001**
Age	32.442	.222
Age^2	-45.678	**.018**
Age^3	27.947	.053
Sex	9.111	.146
ICV	502.530	**<.001**
CA1		
Intercept	729.120	**<.001**
Age	226.468	**<.001**
Age^2	-120.395	**<.001**
Sex	17.975	.067
ICV	587.351	**<.001**
CA2/3		

Intercept	251.240	**<.001**
Age	-62.749	**<.001**
Sex	7.227	.052
ICV	232.916	**<.001**
CA4		
Intercept	326.083	**<.001**
Age	-50.078	**.011**
Sex	5.483	.172
ICV	295.554	**<.001**
GC-DG		
Intercept	370.766	**<.001**
Age	-30.442	.149
Sex	7.663	.089
ICV	313.704	**<.001**
ML		
Intercept	699.541	**<.001**
Age	38.222	.256
Age^2	-51.769	**.034**
Age^3	27.628	.130
Sex	11.898	.138
ICV	550.079	**<.001**
Fimbria		
Intercept	118.896	**<.001**
Age	99.889	**<.001**
Age^2	-41.481	**.011**
Sex	4.895	.147
ICV	185.290	**<.001**
Hippocampal fissure		
Intercept	217.206	**<.001**
ICV	107.204	.131
HATA		
Intercept	63.359	**<.001**
Sex	4.994	**<.001**
ICV	54.358	**<.001**

Hippocampal tail		
Intercept	581.907	**<.001**
Sex	21.282	**.033**
ICV	529.434	**<.001**

Notes. Bold indicates p < .05.

Table 6. Model parameters for fixed effects when including level of general cognitive ability in the best fitting models for whole hippocampus and hippocampal subregion volumes

Region	**B**	**P**
Whole hippocampus		
Intercept	3924.655	**<.001**
Age	-3.352	.984
Age^2	-424.260	**<.001**
Age^3	302.973	**.002**
Sex	278.766	**<.001**
GCA	4.165	.082
Age × GCA	-5.571	.788
Age^2 × GCA	-25.242	.077
Age^3 × GCA	-13.688	.198
Parasubiculum		
Intercept	61.129	**<.001**
Age	-35.298	**<.001**
Sex	3.915	**.001**
GCA	0.013	.835
Age × GCA	0.250	.711
Presubiculum		
Intercept	319.470	**<.001**
Age	-135.823	**<.001**
Sex	20.163	**<.001**
GCA	-0.057	.827
Age × GCA	3.009	.214
Subiculum		
Intercept	467.638	**<.001**
Age	-11.672	.662
Age^2	-72.576	**<.001**
Age^3	54.873	**<.001**
Sex	33.274	**<.001**
GCA	0.500	.154
Age × GCA	1.539	.635
Age^2 × GCA	-4.569	**.042**

Age^3 × GCA	-2.734	.103
CA1		
Intercept	713.034	**<.001**
Age	163.514	**<.001**
Age^2	-162.828	**<.001**
Sex	49.062	**<.001**
GCA	0.830	.122
Age × GCA	7.095	.158
Age^2 × GCA	-4.528	.189
CA2/3		
Intercept	245.720	**<.001**
Age	-83.888	**<.001**
Sex	19.013	**<.001**
GCA	0.568	**.004**
Age × GCA	0.967	.618
CA4		
Intercept	320.313	**<.001**
Age	-76.403	**<.001**
Sex	19.165	**<.001**
GCA	0.695	**.001**
Age × GCA	0.602	.787
GC-DG		
Intercept	364.380	**<.001**
Age	-57.441	**.006**
Sex	22.351	**<.001**
GCA	0.513	**.037**
Age × GCA	0.542	.820
ML		
Intercept	687.289	**<.001**
Age	-12.671	.701
Age^2	-78.680	**.001**
Age^3	56.778	**.003**
Sex	39.175	**<.001**
GCA	0.754	.094

Age × GCA	2.038	.611
Age^2 × GCA	-6.937	**.012**
Age^3 × GCA	-2.543	.218
Fimbria		
Intercept	114.412	**<.001**
Age	86.443	**<.001**
Age^2	-50.670	**.003**
Sex	14.347	**<.001**
GCA	-0.062	.711
Age × GCA	3.458	.176
Age^2 × GCA	-1.378	.467
Hippocampal fissure		
Intercept	217.184	**<.001**
GCA	-0.599	.066
HATA		
Intercept	61.972	**<.001**
Sex	7.791	**<.001**
GCA	0.002	.960
Hippocampal tail		
Intercept	569.507	**<.001**
Sex	49.356	**<.001**
GCA	0.551	.256

Notes. GCA = general cognitive ability. Bold indicates $p < .05$.